

List of Responses

Responds to the Anonymous Referee #1's comments:

Special thanks for your good comments which are very useful for us to improve the paper.

1. Response to comment: Please state the advantages of the both PSO and WSA algorithms, and their performance difference in detail, so that readers can know the motivation that you combine them to coevolve to solve the CNOP. Please use statistical method to demonstrate the better optimization performance of ACPW comparing with the PSO and the WSA in perspective of optimization time and accuracy.

Response: It is really true as Rreview1 suggested that we need to clarify the advantages of the both PSO and WSA algorithms and analyze the the better optimization performance of ACPW. Therefore we have illustrated this in the Section 4.1.

“To evaluate the advantages of the ACPW algorithm, we run the PSO, WSA and ACPW programs 10 times and then compare the maximum, minimum and mean objective values as well as the RMSE.

4.1 The advantages of the ACPW algorithm

Because the statistical analysis results are similar for the two TCs with the two resolutions, we only describe the analysis of Fitow at a resolution of 60 km. Table 3 presents the maximum objective value, the minimum objective value, the mean objective value and the RMSE of the 10 results.

Table 3: The analysis results of the PSO, WSA and ACPW methods.

Algorithm	Maximum Value	Minimum Value	Mean Value	RMSE
PSO	1034.192573	724.086002	900.7488578	0.121400896
WSA	1628.841294	323.7493169	930.9103862	0.431193448
ACPW	2240.275956	1243.377921	1542.505251	0.216750584

In Table 3, the maximum objective value is gained from the ACPW algorithm, and its mean value is also more than the other two algorithms. However, the RMSE of PSO is the smallest, which shows the best stability.

For additional analysis, we draw a box-plot of the 10 results for the PSO, WSA and ACPW algorithms, as shown in Fig. 3.

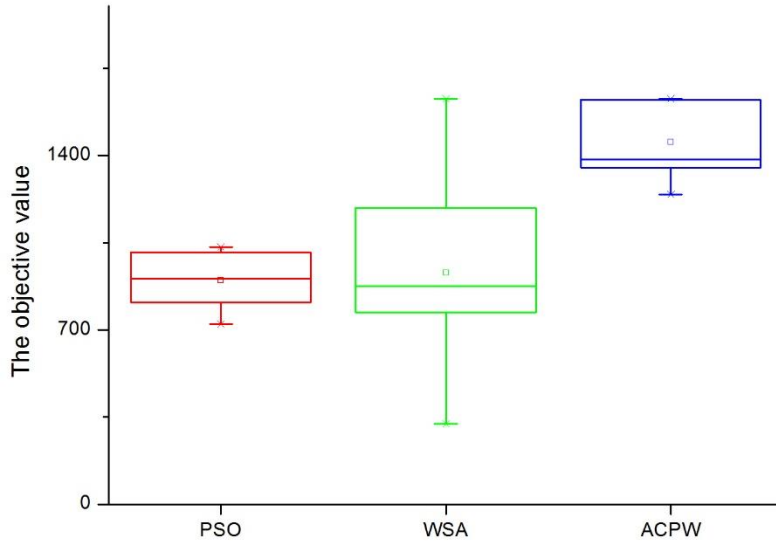


Figure 3: Box-plot of the PSO, WSA and ACPW methods for TC Fitow at 60 km resolution. The red box denotes PSO, the green box is for the WSA, and the blue box shows the results of the ACPW algorithm.

PSO has the narrowest range of values, although the objective values are smaller than the other two algorithms. The WSA has the widest range of values, although the objective values are also smaller than the ACPW algorithm. The ACPW algorithm has the second-best stability, although it has the best objective values. The experiments display the stability of PSO and the exploitation of the WSA. We combine the advantages of them and develop the ACPW algorithm to solve CNOPs. The analysis results demonstrate that the hybrid strategy and cooperation co-evolution is useful and effective.”

2. Response to comment: There is a great difference at the operation rules of the WSA between the standard version given by Rui Tang et al. (2012) and the formula (6) of this study, please make explanation or correction.

Response: We are very sorry about errors in this paper and have corrected them in Page 5, line 2-9. “

$$\begin{cases} u_i^{k+1} = u_i^k + \theta \cdot r \cdot rand() & \text{Prey} \\ u_i^{k+1} = u_i^k + \theta \cdot s \cdot escape() & \text{Escape} \end{cases} \quad (6)$$

where the superscript k or $k + 1$ is also the iterative step, θ is the velocity, r is the local optimizing radius, which is smaller than the global constraint radius δ , $rand()$ is the random function, whose mean value is distributed in $[-1,1]$, $escape()$ is the function for calculating a random position, which is 3 times larger than r , and s is the step size of the updating individual.

As described in Eq. (6), the wolf has two behaviours, i.e., prey and escape. The prey behaviour uses the first sub-formula, and the second one is for the escape function, which happens in every iteration when

the condition $p > p_a$ is satisfied, where p is a random number in $[0,1]$, and p_a is the probability of individual escaping from the current position. ”

3. Response to comment: (1) Page 3, line 24, 26: The variants given in the propagation operator M should be uniform.

Response: As Rreview1 suggested that we rewritten this part in Page 3, line 25.

$$“U_t = M_{t_0 \rightarrow t}(U_0)”$$

4. Response to comment: (2) Page 5, line 8-9: Please state in detail the rule setting adaptive subswarm coefficient α .

Response: As Rreview1 suggested that we have added the rule setting adaptive subswarm coefficient α in Page 5, line13-16.

$$“\alpha = \begin{cases} \alpha + 0.05, & \text{if the bestvalue} - \text{current value} < \varepsilon \\ \alpha - 0.05, & \text{else} \end{cases}”$$

In this paper, before we update the individuals, α is calculated, and then we divide the entire initial swarm into two subswarms according to the α value, i.e., the number of individuals depending on the PSO’s rule is $\alpha \times N$, and the other number is $(1 - \alpha) \times N$. We set the initial value of ε and α to 0.1 and 0.5, respectively. ”

5. Response to comment: (3) Page 5, line 17-19: It is better to delete these three lines since the description is unnecessary.

Response: We need to explain about this part. The reason for writing this part is to present the performance of our algorithms in this paper under those computer hardware environments. If the reader needs to compare with our results, they should have the same environments. Hence, we did not delete them.

In addition, we have improved the quality of our manuscript by American Journal Experts editing service and tracked the changes using revisions in the manuscript ‘Revised Manuscript with Track Changes’.

List of Responses

Responds to the Anonymous Referee #2's comments:

Special thanks for your good comments which are very useful for us to improve the paper.

1. Response to comment: In order to find viable alternatives for using an adjoint, the authors test a combination of two other search algorithms, "particle swarm optimisation" and "wolf search" on a reduced dimension state space with 50 dimension and test their performance against a reference method called "the ADJ method". However, it does not become clear, whether this reference method is used to solve the same problem, which should give identical results provided that all methods find the global minimum. Also, solving a 50-dimensional problem with 200 (resp. 420; see swarm size from table 1) model integrations at each solver step in 20 to 30 steps (Fig. 2) does not look like a dramatic improvement over conventional methods, and no direct comparison to those is offered.

Response: It is really true as Rreview2 suggested that we should give identical results provided that all methods find the global minimum. And we run the PSO, WSA and ACPW programs 10 times and then compare their results. It is commonly known that all intelligent algorithms are stochastic; that is, even when the input is the same in different trials, the output may be different. Hence, it hard to obtain the same result. But we can use the maximum, minimum and mean objective values as well as the RMSE to evaluate the algorithm. Therefore, we have illustrated this in the Section 4.1.

“To evaluate the advantages of the ACPW algorithm, we run the PSO, WSA and ACPW programs 10 times and then compare the maximum, minimum and mean objective values as well as the RMSE.

4.1 The advantages of the ACPW algorithm

Because the statistical analysis results are similar for the two TCs with the two resolutions, we only describe the analysis of Fitow at a resolution of 60 km. Table 3 presents the maximum objective value, the minimum objective value, the mean objective value and the RMSE of the 10 results.

Table 3: The analysis results of the PSO, WSA and ACPW methods.

Algorithm	Maximum Value	Minimum Value	Mean Value	RMSE
PSO	1034.192573	724.086002	900.7488578	0.121400896
WSA	1628.841294	323.7493169	930.9103862	0.431193448

ACPW	2240.275956	1243.377921	1542.505251	0.216750584
------	--------------------	-------------	--------------------	-------------

In Table 3, the maximum objective value is gained from the ACPW algorithm, and its mean value is also more than the other two algorithms. However, the RMSE of PSO is the smallest, which shows the best stability.

For additional analysis, we draw a box-plot of the 10 results for the PSO, WSA and ACPW algorithms, as shown in Fig. 3.

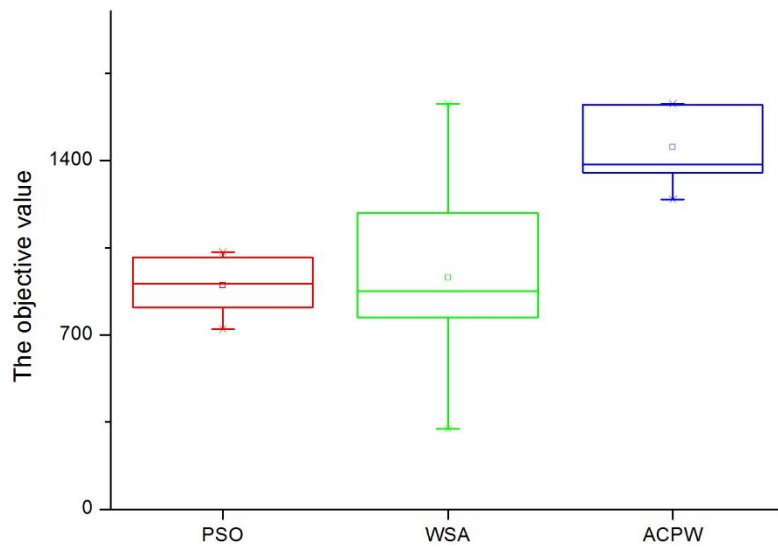


Figure 3: Box-plot of the PSO, WSA and ACPW methods for TC Fitow at 60 km resolution. The red box denotes PSO, the green box is for the WSA, and the blue box shows the results of the ACPW algorithm.

PSO has the narrowest range of values, although the objective values are smaller than the other two algorithms. The WSA has the widest range of values, although the objective values are also smaller than the ACPW algorithm. The ACPW algorithm has the second-best stability, although it has the best objective values. The experiments display the stability of PSO and the exploitation of the WSA. We combine the advantages of them and develop the ACPW algorithm to solve CNOPs. The analysis results demonstrate that the hybrid strategy and cooperation co-evolution is useful and effective.”

2. Response to comment: "The ADJ method" is used as a benchmark, but it is ambiguously defined and no attempts on parallelisation are made, not even in, the case of multiple starting points, which supposedly can be parallelised trivially. Also the article leaves the impression that "the ADJ method" is run on the full state space, rather than the 50 dimensional PC space. In summary, the comparisons in terms of computational performance are not convincing.

Response: As Rreview2 suggested that we inserted the reference of the ADJ-method in L5-6, p.3. “[Specific details of the ADJ-method can be found in Zhou \(2009\).](#)”

As Review2 mentioned that the multiple starting points can be paralleled, but the time consumption will not be less than using one starting point under the same computer hardware environments. When we analyze the efficiency of the ACPW algorithm in Section 4.5, the ADJ-method using one initial guess field (starting point) is compared with the ACPW algorithm. And the speedup of the ACPW reaches 4.53 and 3.84 for the different resolutions.

“To promote the efficiency of the ACPW algorithm, we parallelize it with MPI technology. The time consumption of each case is nearly the same. Hence, we can use one group of experimental results to elucidate the efficiency of the ACPW algorithm. Because the ADJ-method cannot be parallelized because each input depends on the output of the previous step, its time consumption is not changed. Moreover, because this method generally uses 4~8 initial guess fields to obtain the optimal value, we use one and four initial first guess fields to determine the CNOPs. The time consumptions of the ADJ-method and ACPW algorithm are shown in Table 8.

Table8: The time consumption of the ADJ-method and ACPW algorithm (unit: minutes).

Methods	60 km	120 km
ADJ-method (1) ¹	79.9	12.4
ADJ-method (4) ¹	321.1	49.7
ACPW	20.8	2.74

1. ADJ-method (1) means using 1 initial guess field and ADJ-method (4) means using 4 initial guess fields.

At 120 km resolution, the time consumptions of the ADJ-method using 1 and 4 initial guess fields are 12.4 minutes and 49.7 minutes, respectively. At 60 km resolution, the time consumptions are 79.9 minutes and 321.1 minutes, respectively. Unlike the ADJ-method, the ACPW algorithm can be parallelized. When using 22 cores, the ACPW method requires much less time, i.e., 2.74 minutes at 120 km resolution and 20.8 minutes at 60 km resolution. Obviously, the ACPW has higher efficiency. Compared to the ADJ-method (1), the speedup reaches 4.53 and 3.84 for the different resolutions. Compared to the ADJ method (4), the speedup reaches 18.14 and 15.44. Although the different initial guess fields are calculated in parallel, the time consumption must be more than for the ADJ-method (1); the ACPW algorithm is also faster than the ADJ-method.

”

In addition, when the ACPW algorithm calculated the objective value, we use the nonlinear model on the full state space, only update the individual with the 50 dimensions.

3. Response to comment: The experiments with the reduced amplitude CNOPs are hard to follow. I had difficulties to understand section 4.3., which is the motivation for the verification and forecast experiments.

Response: For the Section 4.3, we want to investigate the validity of the sensitive regions identified using CNOPs, and we have two assumptions:

“When adding adaptive observations in sensitive regions, the surrounding environment is idealized, and the improvements from adding observations reduces the original errors by a factor of 0.5.

The obtained CNOPs can be seen as the optimal initial perturbations. Once we reduce them in the

sensitive regions, the benefits are highest.

”

Therefore, we design two groups of idealized experiments. CNOPs are optimal initial perturbations having the maximum nonlinear evolutions at the forecast time. Under these assumptions, by reducing the CNOPs to $W \times \text{CNOPs}$ and inserting them into the initial states we can investigate how the reductions in the CNOPs influence TC forecast skill.

4. Response to comment: In the presentation of the resulting CNOPs, the surface pressure patterns are neither shown nor discussed. No information on the vertical structure of the CNOPs is given. Moisture, an important energy source for tropical cyclones, is not included in the state vector and no justification for this omission is given. The authors do not address the role of the fixed PC space dimension (and basis?) when comparing patterns at different resolutions. No information on how the excitation of numerical modes is avoided, both in the computation of the CNOPs and when making perturbed forecasts.

Response:

As Review2 mentioned that we did not discuss the surface pressure patterns and the vertical structure of the CNOPs, because the purpose of this paper is to identify the adaptive observation sensitive areas, we follow the study of Dr. Zhou that the total dry energy have higher benefits than other strategies (Zhou and Zhang, 2014). Therefore, the information of the surface pressure patterns and the vertical structure of the CNOPs are contained in the total dry energy. In addition, Dr. Zhou has proved that the sensitive regions gained by the dry energy have higher benefits than those obtained from the moist energy (Zhou, 2009). In this paper, we only considered the total dry energy.

For the question that “The authors do not address the role of the fixed PC space dimension (and basis?) when comparing patterns at different resolutions”, the numbers of PCs in this paper are determined by the many experiments, and the analysis of the different numbers are plotted in our previous studies.

Finally, in this paper, we also use the nonlinear model, but avoid using the adjoint model to calculate the gradient.

5. Response to comment: Many formulations in the abstract and the article are confusing on a language level, to name only a few: "...suggest that the use of an ocean coupled model needs to be conscious,..." (page 2, line 13), "the mutual affection of binary typhoons" (page 2 line 14), "[wolf search] ... takes long consuming time." (page 4, line 6). Language editing is encouraged.

Response: As Review2 suggested that we have improved the quality of our manuscript by American Journal Experts editing service and tracked the changes using

revisions in the manuscript ‘Revised Manuscript with Track Changes’.

6. Response to comment: What is the update for u_i if neither of the two conditions is satisfied?

Response: We are very sorry about errors in this paper and have corrected them in L2-9 Page 5. “

$$\begin{cases} u_i^{k+1} = u_i^k + \theta \cdot r \cdot rand() & \text{Prey} \\ u_i^{k+1} = u_i^k + \theta \cdot s \cdot escape() & \text{Escape} \end{cases} \quad (6)$$

where the superscript k or $k + 1$ is also the iterative step, θ is the velocity, r is the local optimizing radius, which is smaller than the global constraint radius δ , $rand()$ is the random function, whose mean value is distributed in $[-1,1]$, $escape()$ is the function for calculating a random position, which is 3 times larger than r , and s is the step size of the updating individual.

As described in Eq. (6), the wolf has two behaviours, i.e., prey and escape. The prey behaviour uses the first sub-formula, and the second one is for the escape function, which happens in every iteration when the condition $p > p_a$ is satisfied, where p is a random number in $[0,1]$, and p_a is the probability of individual escaping from the current position. ”

7. Response to comment: page 8, formula 10: Is this using the same energy norm as formula 10? If not, how are the different variables combined?

Response: formula (10) is used to calculate the similarity between the CNOPs, every CNOP has the same components, so we did not use the norm. Actually, the formula is for solving the Cosine similarity.

样式定义: 批注文字: 字体: (默认) Tahoma, 8 磅, 左, 行距: 单倍行距

A Novel Approach for Solving ~~CNOP~~CNOPs and ~~its~~Its Application in Identifying Sensitive Regions of Tropical Cyclone Adaptive Observations

Linlin Zhang¹, Bin Mu¹, Shijin Yuan¹, Feifan Zhou^{2,3}

5 ¹School of Software Engineering, Tongji University, Shanghai 201804

²Laboratory of Cloud-Precipitation Physics and Severe Storms, Institute of Atmospheric Physics, Chinese Academy of Sciences, Beijing 100029

³University of Chinese Academy of Sciences, No.19 (A) Yuquan Road, Shijingshan District, Beijing 100049

Correspondence to: Shijin Yuan (yuanshijin2003@163.com)

10

Abstract. In this paper, a novel approach is proposed for solving conditional nonlinear optimal ~~perturbation (CNOP), named~~ ~~#~~perturbations (CNOPs), called the “adaptive cooperation co-evolution of parallel particle swarm optimization and wolf (ACPW) search algorithm-(ACPW) based on principal component analysis”. Taking Fitow (2013) and Matmo (2014) as two tropical cyclone (TC) cases, ~~CNOP~~CNOPs solved by ~~the~~ ACPW ~~is~~algorithm are used to investigate the sensitive regions ~~identification of~~identified by TC adaptive observations with the fifth-generation mesoscale model (MM5). Meanwhile, the 60 km and 120 km resolutions are adopted. The adjoint-based method (short for the ADJ-method) is also applied to solve ~~CNOP~~CNOPs, and the result is used as a benchmark. ~~To evaluate the advantages of the ACPW algorithm, we run the PSO, WSA and ACPW programs 10 times and then compare the maximum, minimum and mean objective values as well as the RMSEs, and the analysis results prove that the hybrid strategy and cooperation co-evolution are useful and effective.~~ To

15

validate the ~~validity of~~ ACPW ~~algorithm~~, the CNOPs obtained from the different methods are compared in terms of the patterns, energies, similarities and simulated TC tracks with perturbations. (1) The ACPW ~~algorithm~~ can capture similar CNOP patterns ~~with~~as the ADJ-method, and the patterns of TC Fitow are more similar than TC Matmo. (2) ~~When using the~~At 120 km resolution, similarities between ~~the~~ CNOPs of the ADJ-method and ~~the~~ ACPW ~~algorithm~~ are higher than those ~~using the~~at 60 km ~~resolution~~. (3) Compared to the ADJ-method, although the CNOPs of ~~the~~ ACPW ~~method~~ produce lower energies, they can ~~obtain better~~have improved benefits gained from the reduction of ~~the~~ CNOPs; not only ~~in~~across the entire domain but also in the ~~identified~~ sensitive regions ~~identified~~. (4) The sensitive regions identified by ~~the~~ CNOPs- ~~from the~~ ACPW ~~has~~algorithm ~~have~~ the same influence on the improvements of the TC ~~tracks~~track forecast skills ~~with~~as those identified by ~~the~~ CNOPs- ~~from~~ the ADJ-method. (5) The ACPW ~~method~~ has a higher efficiency than the ADJ-method. All conclusions prove that ~~the~~ ACPW ~~algorithm~~ is a meaningful and effective method for solving ~~CNOP~~CNOPs and can be used to identify sensitive regions of TC

25

30

adaptive observations.

1 Introduction

Tropical ~~eyelone (TC)~~~~iscyclones (TCs)~~ are one of the most frequent and influential natural hazards in the world. An accurate forecast of ~~TC will be~~TCs is conducive to ~~respond to disasters for the~~ response of the government and people. Thus, it is essential to improve TC forecast skills. One effective way is to identify the sensitive regions of TC adaptive observations ~~(called TCAOs for short)~~ (Franklin and Demaria, 1992; Bergot, 1999; Aberson, 2003). Once ~~add~~ observations in sensitive regions ~~are~~ identified and added to reduce initial errors, better forecast will be expected (Bender et al., 1993; Zhu and Thorpe, 2006; Froude et al., 2007). Conditional nonlinear optimal ~~perturbation (CNOP)~~perturbations (CNOPs) proposed by Mu and Duan (2003) is are a nonlinear extension of the linear singular vector (SV) method; and ~~has~~have been applied to study sensitive regions identification of TCAOs successfully (Mu and Zhou, 2009; Qin, 2010; Zhou and Mu, 2011, 2012a, 2012b; Zhou and Zhang, 2014; Qin and Mu, 2012; Qin et al., 2013; Qin and Mu, 2014; Wang et al., 2010; Wang et al., 2013).

Comparing between the sensitive regions ~~of CNOP-identified~~ from CNOPs and ~~the first SV-those~~ identified through SVs, Qin (2010) concludes that the former is more appropriate for TCAOs. Zhou and Mu (2011) use the CNOP method to investigate ~~the~~ different verification areas and how to affect the identification of sensitive regions. ~~Then they study~~They also studied the influence of ~~the~~ different horizontal resolutions (2012a). Moreover, ~~the~~ different ~~times~~ and regime dependency was also is researched (2012b). These research results ~~direct the~~directed further research. Zhou and Zhang (2014) propose three schemes for identifying sensitive regions based on the CNOP method; and recommend ~~that~~ the vertically integrated energy scheme. Moreover, some researchers analyse the sensitivity of dropwindsonde observations on TC predictions, which is identified by can be used in the CNOP method, and conclude that the sensitive regions ~~of CNOP-identified~~ by CNOPs have a positive impact on TC track predictions (Qin and Mu, 2012; Qin et al., 2013). In studies of ~~improvement of improving the~~ sensitivity- CNOP of CNOPs in TC intensity ~~forecast forecasts~~, Qin and Mu (2014) suggest that the use of an ocean-coupled model needs to be ~~conscious, considered~~ as well as the better initialization of the TC vortex. Wang et al. (2013) use the CNOP method to study the mutual affection of binary typhoons. Previous ~~researches studies~~ have proved shown that the CNOP method is a useful and meaningful method for ~~the above~~ study the aforementioned phenomena (Zhou et al., 2013; Mu and Zhou, 2015).

~~Generally, there~~There are generally two ~~type types of~~ methods for solving ~~CNOP, ones~~CNOPs: one based on adjoint models ~~(called ADJ-method for short)~~ and ~~ones one~~ without adjoint models. As useful and effective methods for solving ~~CNOP CNOPs~~ without adjoint models, some modified intelligent algorithms (IAs) based on dimension reduction have been successfully proposed and applied to solve ~~CNOP CNOPs~~ in the Zebiak-Cane (ZC) model ~~successfully~~, such as SAEP-Simulated Annealing Based Ensemble Projecting Method (simulated annealing based ensemble projecting method) (Wen et al., 2014), PPSO-(principal component analysis) (PCA; Jolliffe, 1986)-Based Particle Swarm Optimization)-based particle swarm optimization (Mu et al., 2015a), PCGD-Principal Components (principal components)-based Great Deluge great deluge (Wen et al., 2015a), RGA-Robust (robust PCA-Based Genetic Algorithm)-based genetic algorithm (Wen et al., 2015b), CTS-SS-Continuous (continuous Tabu Search Algorithm)-search algorithm with Sine Maps sine maps and Staged Strategy staged strategy (Yuan et al., 2015), and PCAGA-Principal Component Analysis-Based Genetic Algorithm (principal component analysis-based genetic

algorithm) (Mu et al., 2015b). Compared to the ADJ-method, these methods all can obtain CNOPs with the similar spatial patterns and acceptable objective function values, and several of them have been paralleled with the Message Passing Interface (MPI) and cost less, reducing the computation time consumption. In the TC adaptive observations, such adjoint-free methods are also required urgently, because no having the lack of adjoint models and solution spaces with too high many dimensions of solution space have become obstacles for solving CNOPs, which CNOPs; this is also the focal point of such research in this study.

Actually, we have adopted the PCAGA method to solve CNOPs for the sensitive regions identified by TCAOs with the fifth-generation mesoscale model (MM5) and obtained meaningful results (Zhang et al., 2017). However, we used a resolution we used is of 120 km, which is the lowest in such research. When using a higher resolution, more small-scale information can be achieved predicted, and more accurate sensitive regions can be expected. It is necessary to use a higher resolution. Moreover, although the PCAGA method achieves the meaningful results, its performance is not good enough. It is insufficient because this algorithm is based on a genetic algorithm, which has a good global searching ability but slow convergence rate. In addition, the PCAGA method was not parallelized in the previous study.

Therefore, in this paper, we propose a novel approach, adaptive cooperation co-evolution of PSO and wolf search algorithm (WSA) based on PCA (called ACPW for short) to solve CNOPs for the sensitive regions identified by TCAOs. We take two tropical cyclones as study cases, Fitow (2013) and Matmo (2014), and simulate them with the MM5 model using two different resolutions, 60 km and 120 km. According to the study of Zhou and Zhang (2014), we adopt the total dry energy as the objective function. And the CNOPs from the ADJ-method are referred as a benchmark. Specific details of the ADJ-method can be found in Zhou (2009). To validate the validity of ACPW method, the CNOPs from the ACPW method are compared with the benchmark in terms of the patterns, energies, similarities and benefits from the CNOPs reduced in the entire domain and sensitive regions identified. Further, the CNOPs with different resolutions are also compared in terms of these aspects. Besides, to evaluate the sensitive regions located by the ACPW algorithm, we simulate TC tracks with the initial states perturbed by the amended CNOPs in the location of the sensitive regions from those two methods. And the ACPW algorithm and ADJ-method. Moreover, we design two schemes to amend the CNOPs in the same points and the equivalent proportional points of grids. In addition, we evaluate the efficiency of the ACPW algorithm. All experimental results show that the ACPW method is a meaningful and effective method to solve CNOPs for selecting the sensitive regions of TCAOs.

The organization of the paper is as follows. Section 2 describes the formalized definition of CNOPs and the ACPW method. In section 3, we give the design of the experiments in this study. Section 4 presents the experimental analysis and results. Summaries and conclusions are provided in section 5.

2 Theory and Method

2.1 CNOPs

The mathematical formalism of CNOPs is described as in Eq. (1). Under the constraint condition $\|u_0\|^2 \leq \delta$, an initial perturbation δu_0^* of vector U_0 (initial basic state) is called a CNOP; if and only if

$$J(\delta u_0^*) = \max_{\|u_0\|^2 \leq \delta} J(u_{NT}), \quad (1)$$

where

$$u_{NT} = PM(U_0 + \delta u_0) - PM(U_0), \quad (2)$$

and P represents a local projection operator; the value within the verification region is 1, outside is and 0 elsewhere.

$$U_t = M_{t_0-t}(U_0), \quad (3)$$

where M expresses a nonlinear propagation operator, and U_t is the development of U_0 at time t .

2.2 ACPW method

In this paper, we propose the ACPW method to solve CNOPs for identifying sensitive regions of TCAOs. The core of this approach is the cooperation co-evolution of two intelligent algorithms: PSO and WSA, and the adaptive number of two subswarms. PSO is a classical population-based stochastic optimization technique developed by Eberhart and Kennedy (1995) and inspired by social behaviours of bird flocking or fish schooling; and it has been applied to solve CNOP successfully and effectively applied to solve CNOPs in the ZC model for studying El Niño-Southern Oscillation (ENSO) predictions (Mu et al., 2015a). The WSA is a new bio-inspired heuristic optimization algorithm based on wolf preying behaviours, which was proposed by Rui Tang et al. (2012) and has been applied to study the travelling salesman problem with test functions. Their experiments showed that the WSA is an effective global optimizing algorithm; but needs long consuming time.

We have adopted PSO and the WSA method respectively to solve CNOPs in the MM5 model, but although the results from them exhibit slow convergence or premature convergence. Hence, we combine the advantages of these two algorithms. We use the WSA to explore the global space due to its individuals' independence; and use PSO to dig the local space for making sure and ensure the convergence of the ACPW. Meanwhile, we design the adaptive subswarms of PSO and WSA for cooperation co-evolution. The ACPW framework of ACPW is shown in Fig. 1.

In Fig. 1, the most important part of the ACPW algorithm is inside the dotted box. We divide the entire initial swarm into two subswarms with the same number of individuals; one updates the individuals with the PSO's rule and the other one with the WSA's rule. Then, these two subswarms are adaptively varied along with the convergence state of the ACPW algorithm, i.e., when the change of the objective function adaptive value is less than a threshold value, the number of individuals in the subswarm belonging to the WSA will be increased, and the other subswarm belonging to PSO will decrease

theis decreased by an equal number of individuals to keep the same number ~~offor~~ for the ~~wholeentire~~ swarm. These improvements bring better convergence accuracy and higher evolution velocity, which ~~shewis shown~~ in Fig. 2. The more specific analysis is discussed in ~~Sectionsection~~ 4.

The process of solving ~~ENOPCNOPs~~ with the ACPW ~~algorithm~~ is described as follows:

- 5 1) *Randomly generate an initial swarm with N individuals.* An individual u_i needs to satisfy the boundary constraint in the terms of Eq. (4). Once u_i goes ~~out-ofbeyond~~ the boundary, it must ~~thus~~, be pulled back, i.e.,

$$u_i = \begin{cases} u_i & \|u_i\| \leq \delta \\ \frac{\delta}{\|u_i\|} \times u_i & \|u_i\| > \delta \end{cases} \quad i = 1, \dots, N \quad (4)$$

- 2) *Divide the ~~wholeentire~~ initial swarm ~~into~~ two subswarms with an adaptive coefficient α .* One subswarm updates ~~individualindividuals~~ with the PSO's rule and the other ~~one~~ with the WSA's rule.

- 10 3) *~~Parallely calculate~~Calculate the adaptive value of the objective function ~~in parallel~~, i.e., $J(u_i)$ in Eq. (1).*

- 4) *Update individuals by PSO (Eq. (5)) or ~~the~~ WSA (Eq. (6)).*

$$\begin{cases} v_i^{k+1} = \omega v_i^k + c_1 \alpha (o_i^k - u_i^k) + c_2 \beta (o_g^k - u_i^k) \\ u_i^{k+1} = u_i^k + \gamma v_i^{k+1} \end{cases} \quad (5)$$

where, the superscript k or $k + 1$ is the iterative step, v_i^{k+1} is the velocity of the individual u_i^k and calculated by the first subformula, ω is the inertia coefficient, c_1 and c_2 are the learning factors, α and β are the random numbers uniformly distributing on the interval from 0 to 1, o_i^k is the local optimum ~~and~~, o_g^k is the global optimum in the k^{th} iteration, γ is the restraint factor to control the speed, ~~and~~ u_i^{k+1} is the updated individual ~~withbased on~~ PSO.

- 15 There are two ways for updating ~~individualindividuals~~ in the WSA, i.e., prey and escape, which represent the functions of searching in a local region and escaping from a local optimum:

$$\begin{cases} u_i^{k+1} = u_i^k + \theta \cdot r \cdot rand() \cdot Prey \\ u_i^{k+1} = u_i^k + \theta \cdot s \cdot escape() \end{cases} \quad (6)$$

- 20 $\begin{cases} u_i^{k+1} = u_i^k + \theta \cdot r \cdot rand() \cdot Prey \\ u_i^{k+1} = u_i^k + \theta \cdot s \cdot escape() \end{cases} \quad (6)$

where the superscript k or $k + 1$ is also the iterative step, θ is the velocity, r is the local optimizing radius, which ~~is~~ smaller than the global constraint radius δ , $rand()$ is the random function, whose mean value ~~is~~ distributed in $[-1, 1]$, $escape()$ is the function ~~offor~~ calculating a random position, which is ~~larger-3~~ times ~~larger~~ than r , ~~and~~ s is the step size of the updating individual.

- 25 As the description of ~~described in~~ Eq. (6), ~~the~~ wolf has two behaviours, i.e., prey and escape. The prey ~~behaviour~~ uses the first sub-formula, and the second one is for the escape ~~function~~, which ~~will~~ happens in every iteration; when the condition $p > p_a$ is satisfied, where p is a random number in $[0, 1]$, ~~and~~ p_a is the probability of individual escaping from the current position.

5) Judge whether the change of the adaptive value of the objective function is smaller than ϵ . If yes, set a new value to the adaptive subswarm coefficient α . If not, continue running the process. The updating procedure for α is described as follows:

$$\alpha = \begin{cases} \alpha + 0.05, & \text{if } \text{bestvalue} - \text{current value} < \epsilon \\ \alpha - 0.05, & \text{else} \end{cases} \quad (7)$$

5 In this paper, before we update the individuals, α is calculated first, and then we divide the entire initial swarm into two subswarms according to the α value, i.e., the number of individuals depends on the PSO's rule is $\alpha \times N$, and the other number is $(1 - \alpha) \times N$. We set the initial value of ϵ and α as 0.1 and 0.5, respectively.

6) Judge whether the termination condition is satisfied. If yes, terminate the iteration. Otherwise, go to step 2.

10 All of above processes are based on the dimension reduction within PCA, whose procedure has been described in the study of Mu et al. (2015a). After many experiments, the parameters of the ACPW algorithm can be set as shown in Table-1.

15 Although the parameters are more than for each single algorithm, but most of them still retain the same empirical value of each algorithm, which need and do not to adjust require adjustments. The reason for using a different number of individuals is that the memory of internal storage we used is memory was not enough sufficient when using more than 200 individuals and, resulting in premature termination of the ACPW will be interrupted algorithm.

3 Experiments Design

All the experiments are run on a Lenovo Thinkserver RD430 with two Intel Xeon E5-2450 2.10 GHz CPUs, 32 logical cores and 132G RAM. And the operating system is CentOS 6.5. All the codes are written in FORTRAN language and compiled by PGI Compiler 10.2.

20 3.1 The model and Data

25 In this paper, we adopt the MM5 model to study the sensitive region identification of TCAOs, and the corresponding adjoint system of the MM5 model (Zou et al., 1997) is used to obtain the benchmark. And the ERA interim daily analysis data (1°×1°×1°) (Dee et al., 2011) from the European Center for Medium range Weather Forecasts (ECMWF) are used to generate the initial conditions and boundary conditions. The physical parameterization schemes are defined as follows: dry convective adjustment, the high-resolution planetary boundary layer scheme, grid-resolved large-scale precipitation and the Kuo cumulus parameterization scheme.

We also utilize the best TC track data (Ying et al., 2014) from the China Meteorological Administration - Shanghai Typhoon Institute (CMA-SHTI) as TC tracks observed for evaluating the simulation TC tracks of the MM5 model.

带格式的: 字体: 10 磅

3.2 Typhoons ~~synop to~~ Fitow (2013) and Matmo (2014)

~~TC~~TCs Fitow (2013) and ~~TC~~TC Matom (2014) are taken as the study cases and introduced below. Fitow ~~is was~~ the ~~23st~~23rd TC in 2013; and ~~develops~~developed to the east of the Philippines on 29 September ~~29 and strikes, striking~~ China at Fuding in Fujian ~~province On~~Province on 6 October ~~6~~. Matom ~~is was~~ the 10th named typhoon in 2014, and it ~~happens~~formed on 17 July ~~17 and~~ ~~lands~~made landfall in Taiwan on 22 July ~~22~~. For these two cases, 24-h control forecasts are set as background fields ~~which integrate~~based on integration from 0000 UTC 5 Oct 2013 to 0000 UTC 6 Oct 2013 (TC Fitow) and from 1800 UTC 21 Jul 2014 to 1800 UTC ~~22 Jul~~22 Jul 2014 (TC Matom). After the ~~24h~~24 h period, TC Fitow ~~has the~~had a maximum sustained wind of 162 kilometres per hour ~~and, whereas~~ TC Matmo ~~has had a maximum wind speed of~~ 151.2 kilometres per hour. In addition, the forecasts ~~are were~~ executed at ~~the~~ 60 km and 120 km resolutions with 11 vertical levels, and the model domain ~~covers~~covered 55×55 and 21×26 grids, respectively.

The simulated TC tracks ~~off from the~~ MM5 model for these two cases are acceptable, as has been shown in our previous study (Zhang et al. 2017). The following ~~work will base~~analysis is based on those simulations.

3.3 Experimental setup

~~Depending on the conclusion that a little change of~~Because slight changes in the verification ~~areas~~area never hurts the results (Zhou and Mu, 2011), we design the verification areas as rectangles covering the potential typhoon tracks at ~~the~~ forecast time. The initial perturbation sample δu_0 is composed of the perturbed zonal wind u'_0 , meridional wind v'_0 , temperature T'_0 and surface pressure p'_{s0} . Each component can be represented as ~~a~~ a $m \times n \times l$ matrix, ~~where~~ $m \times n$ is the distribution of the horizontal grid, and l denotes the number of vertical levels. ~~In order to~~To extract features for reducing the dimensions ~~of and~~ solving CNOPCNOPs, the $m \times n \times l$ matrix is reshaped to a $k \times 1$ vector, ~~here where~~ $k = m \times n \times l \times S$ (S is the number of the components). Assuming we have R vectors to represent the features of the solution space, we recombine the R vectors to a $k \times R$ matrix, and use PCA to capture the feature space with lower dimensions. Then, the CNOP is solved in the feature space until ~~we~~ obtain the global CNOP, which will be projected to the original solution space. When using the ACPW ~~algorithm~~ to solve CNOPCNOPs, its initial inputs are produced by the random way in the feature space, and the CNOP has the largest nonlinear evolution at prediction time, i.e., ~~the~~ the largest adaptive value of the objective function in Eq. (9). ~~The objective~~ function is measured by the total dry energy; (Zhou and Zhang, 2014) because Dr. Zhou has proved that the sensitive regions gained by the dry energy ~~had have~~ higher benefits than those obtained from the ~~moisture~~moist energy (Zhou, 2009).

~~There exists~~

The following is defined:

$$f(i, j) = \int_0^1 E_T(i, j, \sigma) d\sigma, \quad (8)$$

where $E_T(i, j, \sigma)$ denotes the total dry energy of ~~the~~ CNOP at the MM5 grid point (i, j, σ) .

Corresponding to formula (1) and (2), we have

带格式的: 字体颜色: 蓝色

带格式的: 英语(英国)

$$J(u_{NT}) = \frac{1}{D} \int_D \int_0^1 \left[u_t'^2 + v_t'^2 + \frac{c_p}{T_r} T_t'^2 + R_a T_r \left(\frac{p_{st}'}{p_r} \right)^2 \right] d\sigma dD, \quad (9)$$

where u_t' , v_t' , T_t' , p_{st}' and p_r' are the components of u_{NT} , which is the nonlinear development of the perturbed U_0 (i.e.: $U_0 + \delta u_0$) from the initial time t_0 to the prediction time t , and σ is the vertical coordinate. And Table 2 illustrates the other reference parameters.

- 5 For the convenience of optimization, solving CNOPCNOPs can be transformed to a minimum problem as follows:

$$J(\delta u_0^*) = \min_{\|u_0\|^2 \leq \delta} \left(-\frac{1}{D} \int_D \int_0^1 \left[u_t'^2 + v_t'^2 + \frac{c_p}{T_r} T_t'^2 + R_a T_r \left(\frac{p_{st}'}{p_r} \right)^2 \right] d\sigma dD \right) \quad (10)$$

To facilitate understanding, all symbols are listed in Table 2, and their meanings are also explained.

4. Experimental Results and Analysis

To evaluate the advantages of the ACPW algorithm, we run the programs of PSO, WSA and ACPW for 10 times, and then compare the maximum, minimum and mean objective values, and as well as the RMSE of them.

4.1 The advantages of the ACPW algorithm

Because the statistical analysis results are similar for the two TCs with the two resolutions, we only describe the analysis of the Fitow with a resolution of 60 km. Table 3 presents the maximum objective value, the minimum objective value, the mean objective value and the RMSE of the 10 results.

- 15 In Table 3, the maximum objective value is gained from the ACPW algorithm, and its mean value is also more than the other two algorithms. However, the RMSE of PSO is the smallest, which shows the best stability.

For additional analysis, we draw the box-plot of the 10 results for the PSO, WSA and ACPW algorithms, as shown in Fig. 3.

- 20 In Fig. 3, we can find that the PSO has the narrowest value range, but of values, although the objective values are smaller than the other two algorithms. The WSA has the widest value range, but of values, although the objective values are also smaller than the ACPW algorithm. The ACPW algorithm has the second-best stability, but although it has the best objective values. The experiments display the stability of the PSO, and the exploitation of the WSA. We combine the advantages of them, and develop the ACPW algorithm to solve the CNOPCNOPs. The analysis results provedemonstrate that the hybrid strategy and cooperation co-evolution is useful and effective strategies.

25 4.2 CNOP patterns

To validate the validity of ACPW algorithm for solving CNOPCNOPs and to identify the sensitive regions, we compare CNOPs the ADJ-method and CNOPs the ACPW algorithm results in terms of the CNOP patterns, energies, similarities, benefits from reduction of the CNOPs, and simulated TC tracks with perturbations.

带格式的: 英语(英国)

In this subsection, we compare the CNOPs obtained from the ADJ-method and the ACPW algorithm in terms of the patterns of temperature and wind. Experimental results show that TC Fitow has more similar CNOP patterns than TC Matmo. The CNOP patterns are described in Fig. 4.

At 120 km resolution for TC Fitow (Fig. 4a, b), the two methods have almost the same major warm locations and similar cold parts, while the wind vectors have opposite directions. The ADJ-method captures the CNOP with two major locations. The red (warm) one is distributed to the west of the initial cyclone (called IC for short), and the green (cold) one is distributed to the north of the IC. The ACPW algorithm also captures the CNOP with two main locations. The warm one is distributed to the west, and the cold one is located at the northwest of the IC. In this subsection, the spatial orientation is relative to the position of the IC. Therefore, in the following discussion, we explain the spatial orientation in the figures without repeating the IC.

For TC Fitow with the 60 km resolution (Fig. 4c, d), the CNOP spatial distribution based on the ACPW algorithm is very similar to the ADJ-method's results. In the northwest of the verification area, the two CNOPs have two similar major parts, one warm area and one cold area. The difference between these two patterns is that the ADJ-method has another major warm area located in the northwest and, while the ACPW method produces another major warm area located in the east. Besides, the distribution of the secondary parts shows only a slight difference.

For the same method with the different resolutions (Fig. 4a, c and Fig. 4b, d), the CNOP patterns have similar major distributions in the northwest, but with within a different region. The reason is that when using a higher resolution, more small-scaled things will be resolved (Zhou and Mu, 2012a).

For TC Matmo with the 120 km resolution (Fig. 5a, b), the ADJ-method and ACPW algorithm obtain CNOPs with different spatial patterns in terms of temperature and wind. The ADJ-method has two major parts, with the warm one located in the west and the cold one distributed in the east. The ACPW algorithm results in two main parts distributed in the northeast with one warm area near the IC and a cold one far from the IC. For TC Matmo with the 60 km resolution (Fig. 5c, d), in the verification area, the two CNOP patterns have similar spatial distributions, with two warm areas located at nearly the same positions. But, however, the parts outside of the verification area are distributed in the different positions. Besides, moreover, the CNOP of the ADJ-method has more regular distributions than the ACPW's distributions. For the same method with the different resolution (Fig. 5a, c and Fig. 5b, d), the CNOP patterns cover similar areas but with different ranges and details.

Based on the above analysis about the patterns of temperature and wind, we can conclude that when using the resolution of 60 km, the CNOPs of the ADJ method predicted by the ADJ method and ACPW algorithm have more similar major patterns than those with the predicted at a resolution of 120 km. In addition, the ACPW algorithm can obtain CNOPs with more similar patterns in TC Fitow than in TC Matmo.

Vertically integrated energies of the CNOPs for TC Fitow are displayed in Fig. 6. Compared to the ADJ-method, when using the 120 km resolution, the CNOPs of the ACPW method have much lower energy and various differing positions.

but. However, when using 60-km resolution, it can get of 60 km, similar energies and positions. Besides are obtained. Moreover, the energy of the CNOPs obtained from the ACPW algorithm has a larger range in the center. Vertically integrated energies of the CNOPs for TC Matmo are displayed in Fig. 7. Compared with the ADJ-method, when using the at 120 km resolution, the CNOPs of the ACPW algorithm have a lower energy and covers large cover larger areas. but. However, when using the 60-km resolution of 60 km, although the energy is still lower, but the positions are getting closer more similar.

4.2 Similarities

When we evaluate the CNOPs, in addition to the characteristics and distributions of the CNOP patterns, consideration should also be given to numerical similarities and to the benefits from of the CNOPs. Therefore, we calculate the similarity between the CNOPs determined from the ADJ-method and the ACPW algorithm and use X and Y to represent them in the formula (10).

$$S_{xy} = \frac{\langle X, Y \rangle}{\sqrt{\langle X, X \rangle} \sqrt{\langle Y, Y \rangle}} \quad (10)$$

The results are shown in Table. 4. The similarity values can reflect the similarities among the CNOP patterns of CNOPs (Fig. 4 and Fig. 5).

In Table. 4, for TC Fitow, the similarity with the at 120 km is -0.83, and whereas that with the 60-km resolution of 60 km is 0.43. For TC Matmo, the similarity with the at 120 km is 0.42, whereas that with a resolution is 0.42, and that with the of 60 km resolution is 0.37. The negative sign represents indicates that parts of the CNOPs from these two methods have opposite wind vector directions, which is shown in Fig. 4. We also find that when using a higher resolution, the similarity is lower. The reason for this finding is that although the major patterns of the CNOPs are similar, the other secondary parts of them are different, differ and they cover larger areas. Actually, when using a higher resolution, we can achieve more small-scale information, and the identification of sensitive regions becomes more accurate. As Regarding the analysis of the CNOP patterns, we assuredly get obtain more similar major patterns when using the for a resolution of 60 km resolution than using the 120 km resolution, but. However, compared with the other different parts, the similar parts are very small. However, the decreased similarities decreased will do not affect identifying the sensitive regions, because the adaptive observations only focuses focus on the points with bigger influence larger influences, which will be proved in demonstrated subsection 4.4 of this section.

We also compare the energy for 24 hours of nonlinear development under the initial states perturbed by different CNOPs, i.e., $J(M(U_0 + \delta u_0^*))$. The results are shown in Table. 5.

Results show that all CNOPs obtained using the ACPW produce lower energies than the those of the ADJ-method, but. However, when reducing the CNOPs to W-CNOPs in the entire domain and reducing the CNOPs to by a factor of 0.5 in the sensitive regions identified, the ACPW algorithm has better benefits results, which will be discussed in following subsection.

带格式的: 英语(英国)

4.3 Benefits from ~~Reduction of~~Reducing the CNOPs

In this subsection, we design two groups of idealized experiments to investigate the validity of ~~the~~ sensitive regions identified by ~~using~~ CNOPs, based on ~~two~~the following assumptions ~~that~~:

When adding adaptive observations in sensitive regions ~~identified~~, the ~~surrounding~~ environment ~~around~~ is idealized, and the improvements ~~offrom adding~~ observations ~~added are reducing~~reduces the original errors ~~to by a factor of~~ 0.5 ~~times~~.

~~The obtained~~ CNOPs ~~achieved by us~~ can be seen as the optimal initial perturbations. Once we reduce them in the sensitive regions, the benefits ~~earned will be the best~~are highest.

Under ~~the above~~these assumptions, ~~by~~ reducing the CNOPs to $W \times$ CNOPs and inserting them ~~to into~~ the initial states ~~we~~ can investigate ~~how~~ the reductions ~~of in the~~ CNOPs ~~how to~~ influence TC forecast ~~skills~~. ~~Besides~~skill. ~~Moreover~~, reducing the ~~values of~~ CNOPs ~~to by a factor of~~ 0.5 ~~time~~ in the ~~identified~~ sensitive regions ~~identified~~ by vertically integrated ~~the~~ energies can ~~be used~~ investigate ~~that adding~~how the addition of adaptive observations in the sensitive regions ~~how to can~~ impact ~~on~~ TC forecast ~~skills~~skill.

~~First, as~~ CNOP ~~because~~ CNOPs can be seen as the optimal initial perturbations in the TCAOs, we reduce ~~CNOP~~the CNOPs to $W \times$ CNOP, ~~where~~ W is a coefficient in $(0, 1)$, and insert ~~CNOP~~the reduced CNOPs into the initial state ~~with and allow for~~ 24-h ~~of~~ evolution of the ~~nonlinear model of the~~ MM5 model, ~~then~~. ~~Then, we~~ calculate the forecast error ~~with using~~ formula (11) to ~~gain~~ determine the benefits ~~from such of the~~ reductions. Second, we determine the sensitive regions ~~with via~~ vertically integrated energies using two schemes: the same points ~~of energies~~ in the different resolutions, and the equivalent percentage of points ~~offrom~~ the different grids. ~~Then,~~ we reduce ~~the~~ CNOPs ~~to by a factor of~~ 0.5 ~~time~~ only in the sensitive regions and insert ~~CNOPs~~the amended ~~to~~ CNOPs into the initial states ~~with~~. ~~The model is run for~~ 24-h ~~evolution of the nonlinear model~~.

The experimental results are ~~denoted~~described below.

4.3.1 Reducing CNOP to $W \times$ CNOPs in the entire domain

~~In this part, we explore the forecast improvement extents of reducing the~~ CNOPs to $W \times$ CNOPs in the entire domain

~~We explore the forecast improvements induced by reducing the CNOPs to $W \times$ CNOPs for the entire domain. The scheme is inserting CNOP approach requires using the reduced~~ ~~into~~ CNOPs in the initial state ~~with for a~~ 24-h ~~evolution of the nonlinear model simulation~~ of the MM5 model. The prediction error is computed by ~~the~~ formula (11):

$$J_1(u_{NT}) = \|PM(U_0 + \delta u_0) - PM(U_0)\|^2, \quad (11)$$

~~Where~~where the definitions of u_{NT} , P , M and U_0 are the same ~~with these as~~ in Eq. (1), (2) and (3).

~~And the~~The prediction error after reducing ~~CNOP in the~~ CNOPs for the entire domain is computed by ~~the~~ formula (12):

$$J_2(u_{NT}) = \frac{\|PM(U_0 + W\delta u_0) - PM(U_0)\|^2}{\|PM(U_0 + W\delta u_0) - PM(U_0)\|^2}, \quad (12)$$

where W is the weighting coefficient, ~~and it which~~ is set ~~as to~~ 0.25, 0.5 or 0.75 for decreasing error. ~~And the~~The benefit from such reductions is calculated by ~~the~~ formula (13):

带格式的: 英语(英国)

带格式的: 英语(英国)

带格式的: 英语(英国)

带格式的: 英语(英国)

带格式的: 英语(英国)

带格式的: 英语(英国)

$$\frac{J_1(u_{NT}) - J_2(u_{NT})}{J_1(u_{NT})} \quad (13)$$

Obviously, the prediction benefit is increasing when W gets increases for decreasing W . Fig. 8 and Fig. 9 also show that the ACPW algorithm can obtain CNOPs with better benefits from reducing the CNOPs to $W \times$ CNOPs infor the entire domain than the ADJ-method, except for thewhen W is 0.25 for TC Fitow with the 60 km at a resolution. The reason of 60 km. This is thatbecause the ACPW algorithm optimizes in a low-dimensional feature space fromdue to the PCA, and focuses on more effective points in the entire domain, which has positive effects on improving the forecast.

4.3.2 Reducing CNOP to the CNOPs by a factor of 0.5 time in the sensitive regions

In this part, we explore the forecast improvement extent which gained from caused by reducing the CNOPs to by a factor of 0.5 time in the sensitive regions. We determine the sensitive regions withbased on vertically integrated energies using two schemes: the 20 biggest points of with the highest energy inat the different resolution, resolutions and the 1/100 points of the different grids, which is 30 points in theat 60 km resolution (55×55) and 6 points in theat 120 km resolution (21×26). The sensitive regions with the 20 biggest points of having the highest energy are denoted in Fig. 10 and Fig. 11.

In Fig. 9 and Fig. 10, we can see that when the equivalent points are approach is adopted, a bigger larger scope is covered with the 120 km resolution than with the 60 km resolution. When using the 20 points from the ADJ-method and ACPW as the sensitive regions algorithm and reducing the CNOPs to by a factor of 0.5 time in these points, the benefits are displayed in Table. 6.

In Table. 6, for TC Fitow, compared to the ADJ-method, i.e., 5.93% in theat 120 km resolution and 3% in theat 60 km resolution, the ACPW algorithm obtains a higher benefit (8.05%) in the for a resolution of 120 km resolution, and a lower benefit (-0.84%) in the for a resolution of 60 km resolution. Here, -0.84% means that a reduction of CNOP cannot obtain in the CNOPs results in no benefit, but and narrows the quality of the initial state. For TC Matmo, the ACPW algorithm achieves a much higher benefit (20.48%) than the ADJ-method's (6.12%) in theat 60 km resolution, while a lower benefit (16.26%) than the ADJ-method's (20.90%) in theat 120 km resolution. In addition, when using the same number of energy points, the benefits in the using 120 km resolution are almost higher than nearly as high as those in the for 60 km resolution, except for the benefit of ACPW in the algorithm at 60 km resolution for TC Matmo.

The sensitive regions with the 1/100 points of from the different grids are denoted in Fig. 12 and Fig. 13.

Fig. 12 and Fig. 13 shows show that when using the different resolutions, the sensitive regions identified by the same method are different. And the The sensitive regions identified by the ACPW algorithm are more dispersive than those identified by the ADJ-method, which is attributed to randomness of the intelligent algorithms. Table. 7 shows the benefits gained from reducing the CNOPs to by a factor of 0.5 time in the sensitive regions identified by the ADJ-method and ACPW algorithm with different points in the different resolutions.

According to Table. 7, for TC Fitow, the ACPW algorithm achieves a 4.23% benefit, which is higher than the ADJ-method (3.9%) in theat 60 km resolution, and a lower benefit 0.01% than the ADJ-method (1.72%) in theat 120 km resolution. For TC

Matmo, the ACPW [algorithm](#) also has a higher benefit (9.75%) and a lower benefit (6.86%) than the ADJ-method (1.21% and 13.24%, respectively).

Combined with Table- 6 and Table- 7, we can conclude that the sensitive regions cover [bigger a larger](#) scope, [and](#) higher benefits [will be are](#) obtained. When using the same proportion of grids with the different resolutions, the sensitive regions under [the](#) higher [resolutions will resolution](#) achieve [the](#) higher benefits. These results also [provedemonstrate](#) that [the](#) CNOPs obtained from the ACPW [algorithm](#) can identify sensitive regions with higher benefits [in the at](#) 60 km resolution.

4.4 Simulated TC Tracks

[To We further](#) investigate the validity of the sensitive regions identified by [CNOP further, we compare the CNOPs using a comparison of](#) simulated TC tracks [of predicted by](#) the MM5 model for each case [with by](#) inserting [the](#) CNOPs or W×CNOPs into the initial states, [and; we](#) also simulate [the](#) TC tracks [with by](#) inserting [CNOPs amended CNOPs](#) in the different sensitive regions (20 or 30 points). [As Because](#) 120 km is the lowest resolution in [such this](#) research, and the tracks cannot be drawn under this resolution in our study, we only analyse the simulated TC tracks [with the at](#) 60 km resolution. [To demonstrate clearly, we We](#) draw two tracks in a subfigure, which are [the](#) observed TC track from the CMA-SHTI and [the](#) simulated TC track from the MM5 model [with overlaying](#); the different perturbations [are overlaid](#) onto the same initial states. According to the experimental results, when overlaying the CNOPs or amended CNOPs onto the same initial states, although the CNOPs are obtained from [the](#) different methods, the simulated tracks are the same. Therefore, we only [exhibit discuss](#) one group of figures for each case. The results are presented in Fig. 14 and Fig. 15.

Fig. 14 demonstrates the simulated TC tracks of the MM5 [with by](#) inserting [CNOP the CNOPs](#) or W×CNOP into the initial state for TC Fitow [and; the](#) four subfigures are the same. The reason is that the deviations between the simulated TC [track and the](#) observed TC track [is are](#) very small; it is not easy to make improvements. Hence, when inserting different CNOPs into [the](#) identical initial states to simulate TC tracks, [the a](#) change is not evident. [Besides Moreover](#), the resolution we used [is the was](#) 60 km, which is not high enough to show more details about changing tracks.

Fig. 15 demonstrates the simulated TC tracks [off from the](#) MM5 [with model by](#) inserting [CNOP the CNOPs](#) or W×CNOP into the initial state for TC Matmo. [Subfigure Subfigures](#) (a) and (b) are the same, and from (b) to (d), the simulated positions after 24 hours are getting closer to the observed positions. [It illustrates These results illustrate](#) that when [the](#) CNOPs [achieved obtained](#) by the ACPW [algorithm](#) and ADJ-method [being seen are used](#) as the optimal initial perturbations, reducing [the](#) CNOPs [have has a](#) positive [effect effect](#) on the forecast [skills skill](#) of the simulated tracks. [And that also proves Moreover](#), the ACPW [algorithm](#) is a meaningful and effective method for solving the approximate [CNOP CNOPs](#) of the ADJ-method.

We also simulate TC tracks [with by](#) inserting the amended CNOPs, which are reduced [to by a factor of 0.5 time in](#) only [in the](#) sensitive regions. [And we We](#) use 20 and 30 points as the sensitive regions to study [such difference how to affect the number of points affects](#) the forecast [skills. And the skill. The](#) results are shown in Fig. 16 and Fig. 17.

In Fig. 16 and Fig. 17, the simulated TC tracks are the same; [for](#) not only [the](#) different [method methods](#) but also [the](#) different sensitive regions. We can conclude that the ACPW [algorithm](#), an adjoint-free method, is a meaningful and effective method

for solving the approximate CNOPs of the ADJ-method. According to these results, we can also conclude that using 20 or 30 points as the sensitive regions, results in the same improvements are achieved in the TC tracks in terms of forecast skills, so that we can use skill. Thus, fewer points can be used in the real adaptive observations to reduce costs.

4.5 The efficiency of the ACPW algorithm

- 5 To promote the efficiency of the ACPW algorithm, we parallelize it with MPI technology. The time consumption of each case is nearly the same almost. Hence, we can use one group of experimental results to elucidate the efficiency of the ACPW algorithm. Because the ADJ-method cannot be parallelized because of its each input depending depends on the output of the previous step, its time consumption is not changed. And as Moreover, because this method generally uses 4~8 initial guess fields to obtain the optimal value, we use one and four initial first guess fields to achieve CNOP-determine the
- 10 CNOPs. The time consumption of the ADJ-method and ACPW algorithm are shown in Table- 8.
1. ADJ-method (1) means using 1 initial guess field, and ADJ-method (4) means using 4 initial guess fields.
- When using the At 120 km resolution, the time consumption of the ADJ-method using 1 and 4 initial guess fields are 12.4 minutes, and 49.7 minutes, respectively. And when using the At 60 km resolution, the time consumption is 79.9 minutes, and 321.1 minutes, respectively. Unlike the ADJ-method, the ACPW has been parallelized, and when algorithm can be parallelized. When using 22 cores, the ACPW method requires much less time, i.e., 2.74
- 15 minutes for the at 120 km resolution and 20.8 minutes for the at 60 km resolution. Obviously, the ACPW has higher efficiency when using the different resolutions. Compared to the ADJ-method (1), the speedup reaches 4.53 and 3.84 for the different resolutions. Compared to the ADJ-method (4), the speedup reaches 18.14 and 15.44. Although the different initial guess fields are calculated in parallel, the time consumption must be more than for the ADJ-method (1); the ACPW algorithm is also faster
- 20 than the ADJ-method.

5 Summaries and Conclusions

- In this study, we present a novel approach, adaptive cooperation co-evolution of paralleled PSO and WSA (ACPW), to solve CNOPs. And the CNOPs based on the ACPW algorithm are applied to study sensitive regions region identification of TCAs in the MM5 model, without using the an adjoint model. We study two TC cases, Fitow (2013) and
- 25 Matmo (2014), with 60 km and 120 km resolutions. The objective function is set as the total dry energy, which is the based on 24 hours nonlinear development of hour simulations starting with initial perturbations at the prediction time within the verification area. We also calculate CNOPs with the ADJ-method and the result is seen; these results are used as a benchmark. To validate the validity of ACPW algorithm, the CNOPs obtained from the different methods are compared in terms of the patterns, energies, similarities, benefits of reduction of CNOPs and simulated TC tracks with perturbation the
- 30 CNOPs and simulated TC tracks with perturbations. To evaluate the advantages of the ACPW algorithm, we run the PSO.

WSA and ACPW programs 10 times and compare the maximum, minimum and mean objective values as well as the RMSE; the analysis results demonstrate that the hybrid strategy and cooperation co-evolution are useful and effective.

According to all of the experiments, we can get the following five conclusions as follows are obtained:

(1) Compared with the ADJ-method, the ACPW algorithm can obtain CNOPs with more similar patterns of temperature and wind for TC Fitw than those for TC Matmo.

(2) When using the 120 km resolution, the similarities of the CNOPs achieved by the ADJ-method and the ACPW algorithm are higher than those using the 60 km. The reason is that although the major patterns of these CNOPs are similar, the other parts of them are different, which differ and cover larger areas. Actually, when using a higher resolution, we can achieve more small-scale information and, moreover, sensitive regions identification will become more accurate. As regarding the analysis of CNOP patterns, we assuredly get more similar major patterns when using the 60 km resolution than using the 120 km resolution, but, although the similar parts are very small compared with the other different parts. However, the decreased similarities will do not affect identifying sensitive regions; because the adaptive observations only focus on the points with bigger influence.

(3) Under the assumptions that when adding adaptive observations in the sensitive regions identified, the environments around for a surrounding environment that is idealized, and the improvements of observations added are reducing the original errors to be reduced by a factor of 0.5 time; the CNOPs achieved by us can be seen as the optimal initial perturbations, once we reduce them. Once they are reduced in the sensitive regions, the benefits earned will be the best are highest. We design two groups of idealized experiments to investigate the validity of the sensitive regions identified by the CNOPs for TC track forecast skill: reducing CNOPs to W×CNOPs and reducing the values of CNOPs to by a factor of 0.5 time in the sensitive regions identified using the vertically integrated energies. The experimental results show that the CNOPs of the ACPW algorithm produce lower energies than the ADJ-method; but can obtain better benefits when reducing the CNOPs in the above two ways.

(4) The ACPW algorithm can gain the effective CNOPs effect for identifying the sensitive regions, which have the same influence on the forecast improvements of the simulated TC tracks with the ADJ-method. We compare the different forecast improvements of the TC tracks earned from the different reduced perturbations, including reducing the CNOPs to W×CNOPs in for the entire domain and reducing the CNOPs to by a factor of 0.5 time in the sensitive regions. The experimental results all support our conclusions.

(5) The ACPW algorithm has a higher efficiency than the ADJ-method. Compared to the ADJ-method using 1 initial guess field, the speedup reaches 4.53 for the 120 km resolution and 3.84 for the 60 km resolution. Compared to the ADJ-method using 4 initial guess fields, the speedup reaches 18.14 and 15.44, respectively.

All of the conclusions prove demonstrate that the ACPW algorithm is a meaningful and effective method for solving approximate CNOPs and identifying sensitive regions of TCAOs. In addition, as we reduce the dimensions with PCA, the CNOPs obtained by us will lose some energies. Compared to the CNOPs from the ADJ-method, the CNOPs from the ACPW algorithm are all local CNOPs. But in However, for the ACPW algorithm, they are the global CNOPs.

Since ~~Because~~ PCA makes our optimization ~~foeusing~~focus on more effective points with higher energies, ~~that~~ the ACPW algorithm can achieve the CNOPs ~~bringing the~~with better benefits and the same ~~influence on the~~improvements ~~of the~~on TC ~~track~~track forecast ~~skills~~skill.

We are restricted to computation sources for the time being, ~~which~~. We are also ~~limits~~limited by the parallelization of the ACPW algorithm. We will improve the computation conditions; and use the parallel ACPW algorithm to solve ~~ENOP~~CNOPs in the weather research forecast (WRF) model with a finer grid and higher ~~resolutions~~resolution. In addition, we will apply this ~~type of~~ method to solve ~~ENOP~~CNOPs in the community earth system model (CESM) model, which does not have an adjoint model.

10 **Acknowledgments:** In this paper, the research was sponsored by the Foundation of National Natural Science Fund of China (No.41405097).

References

- Aberson, S. D.: Targeted Observations to Improve Operational Tropical Cyclone Track Forecast Guidance, *Mon. Wea. Rev.*, 131(131), 1613, 2003.
- 15 Bender, M.A., Ross, R.J., and Tuleya, R.E., Kurihara, Y.: Improvements in tropical cyclone track and intensity forecasts using the GFDL initialization system, *Mon. Wea. Rev.*, 121, 2046–2061, 1993.
- Bergot T.: Adaptive observations during FASTEX: A systematic survey of upstream flights, *Quart. J. Roy. Meteor. Soc.*, 125(561), 3271-3298, 1999.
- Dee, D. P., and 35 co-authors.: The ERA-Interim reanalysis: Configuration and performance of the data assimilation system, *Quart. J. Roy. Meteor. Soc.*, 137, 553-597, 2011.
- 20 Franklin, J. L., and Demaria, M.: The Impact of Omega Dropwindsonde Observations on Barotropic Hurricane Track Forecasts, *Mon. Wea. Rev.*, 120(120), 381-391, 1992.
- Froude, L. S. R., Bengtsson, L., Hodges, K. I.: The Predictability of Extratropical Storm Tracks and the Sensitivity of Their Prediction to the Observing System, *Mon. Wea. Rev.*, 135(2), 315-333, 2007.
- 25 Jolliffe, I. T.: *Principal Component Analysis*, Springer Berlin, 87(100), 41-64, 1986.
- Kennedy, J., and Eberhart, R.: Particle swarm optimization, in: *Proc. of IEEE Int. Conf. Neural Networks*, 1942–8, 1995.
- Mu, B., Wen, S., Yuan, S., and Li, H.: PPSO: PCA based particle swarm optimization for solving conditional nonlinear optimal perturbation, *Comput. Geosci.*, 83, 65-71, 2015a.
- Mu, B., Zhang, L., Yuan, S., and Li, H.: PCAGA: principal component analysis based genetic algorithm for solving conditional nonlinear optimal perturbation, in: *2015 International Joint Conference on Neural Networks (IJCNN)*, IEEE, Ireland, 12-17 July 2015, 1-8, 2015b.
- 30

- Mu, M., and Duan, W. S.: A new approach to studying ENSO predictability: Conditional nonlinear optimal perturbation, *Chinese Sci. Bul.*, 48, 1045-1047, 2003.
- Mu, M., and Zhou, F. F.: The Research Progress of the Typhoon Targeted Observations Based on CNOP Method, *Adv. Meteor. Sci. Technol.*, 3, 6-17, 2015.
- 5 Mu, M., Zhou, F., and Wang, H.: A Method for Identifying the Sensitive Areas in Targeted Observations for Tropical Cyclone Prediction: Conditional Nonlinear Optimal Perturbation, *Mon. Wea. Rev.*, 137(5), 1623-1639, 2009.
- Qin, X. H.: A Comparison Study of the Contributions of Additional Observations in the Sensitive regions Identified by CNOP and FSV to Reducing Forecast Error Variance for the Typhoon Morakot, *Atmos. & Ocean. Sci. Lett.* 03(05), 258-262, 2010.
- Qin, X., Duan, W., and Mu, M.: Conditions under which CNOP sensitivity is valid for tropical cyclone adaptive observations, *Quart. J. Roy. Meteor. Soc.*, 139(675), 1544-1554, 2013.
- 10 Qin, X., and Mu, M.: Can Adaptive Observations Improve Tropical Cyclone Intensity Forecasts?, *Adv. Atmos. Sci.*, 31(2), 252-262, 2014.
- Qin, X.H., and Mu, M.: Influence of conditional nonlinear optimal perturbations sensitivity on typhoon track forecasts, *Quart. J. Roy. Meteor. Soc.*, 662(138), 185-97, 2012.
- 15 Tang, R., Fong, S., Yang, X. S., and Deb, S.: Wolf search algorithm with ephemeral memory, in: Seventh International Conference on Digital Information Management, University of Macau, Macau, June 2012, 165-172, 2012.
- Wang, X. L., Zhou, F. F., and Zhu, K. Y.: The application of conditional nonlinear optimal perturbation to the interaction between two binary typhoons fengshen and fung-wong., *J. Trop. Meteorol.*, 29(2), 235-244, 2013.
- Wang, X., Zhum K., and Zhou, F.: The Study of Conditional Nonlinear Optimal Perturbation'S Application in Typhoon Over the South China Sea (in Chinese), *Tournal of Chengdu University of Information Technology*, 6(25), 640-646, 2010.
- 20 Wen, S., Yuan, S., Mu, B., Li, H., and Chen L.: SAEP: Simulated Annealing Based Ensemble Projecting Method for Solving Conditional Nonlinear Optimal Perturbation, in: Algorithms and Architectures for Parallel Processing, 14th international conference, ICA3PP 2014, Dalian, China, 24-27 August 2014, 655-668, 2014.
- Wen, S., Yuan, S., Mu, B., Li, H., and Ren, J.: PCGD: Principal components-based great deluge method for solving CNOP, *in: Evolutionary Computation (CEC), 2015 IEEE Congress on. IEEE*, 25-28 May 2015, 1513-1520, 2015a.
- 25 Wen, S., Yuan, S., Mu B, and Li, H.: Robust PCA-Based Genetic Algorithm for Solving CNOP, in: Intelligent Computing Theories and Methodologies, 11th International Conference, ICIC 2015, Fuzhou, China, 20-23 August 2015, 597-606, 2015b.
- Ying, M., Zhang, W., Yu, H., Lu, X., Feng, J., Fan, Y., Zhu, Y., and Chen, D.: An overview of the China Meteorological Administration tropical cyclone database, *J. Atmos. Oceanic Technol.* (31), 287-301, 2014.
- 30 Yuan, S., Qian, Y., and Mu, B.: Paralleled Continuous Tabu Search Algorithm with Sine Maps and Staged Strategy for Solving CNOP, in: Algorithms and Architectures for Parallel Processing, 15th International Conference, ICA3PP 2015, Zhangjiatie, China, 18-20 November 2015, 281-294, 2015.
- Zebiak, S.E., Cane, M.A.: A Model El Niño-Southern Oscillation. *Mon. Wea. Rev.*, 10(115), 2262-2278, 1987.

Zhang, L. L., Yuan, S. J., Mu, B., and Zhou F. F.: CNOP-based sensitive areas identification for tropical cyclone adaptive observations with PCAGA method, Asia-Pac. J. Atmos. Sci., 53(1), 63-73, 2017.

Zhou Feifan. Application of conditional nonlinear optimal perturbation method to typhoon target observation. Institute of Atmospheric Physics, Chinese Academy of Sciences, 2009.

5 Zhou, F., and Mu, M.: The impact of verification area design on tropical cyclone targeted observations based on the CNOP method, Adv. Atmos. Sci., 28(5), 997-1010, 2011.

Zhou, F., and Mu, M. The Impact of Horizontal Resolution on the CNOP and on Its Identified Sensitive Areas for Tropical Cyclone Predictability, Adv. Atmos. Sci., 29(01), 36-46, 2012a.

10 Zhou, F., and Mu, M.: The Time and Regime Dependencies of Sensitive Areas for Tropical Cyclone Prediction Using the CNOP Method, Adv. Atmos. Sci., 29(04), 705-716, 2012b.

Zhou, F., Qin, X., Chen, B., and Mu, M.: The Advances in Targeted Observations for Tropical Cyclone Prediction Based on Conditional Nonlinear Optimal Perturbation (CNOP) Method, in: Data Assimilation for Atmospheric, Oceanic and Hydrologic Applications (Vol. II), Springer Berlin Heidelberg, 577-607, 2013.

15 Zhou, F., and Zhang, H.: Study of the Schemes Based on CNOP Method to Identify Sensitive Areas for Typhoon Targeted Observations, Chinese J. Atmos. Sci. (2), 261-272, 2014.

Zhu, H., and Thorpe, A. Predictability of Extratropical Cyclones: The Influence of Initial Condition and Model Uncertainties, J. Atmos. Sci., 63(5), 1483-1497, 2006.

Zou, X. F., Vandenberghe, M. Pondeva, and Kuo, Y-H.: Introduction to adjoint techniques and the MM5 adjoint modeling system, NCAR Tech. Note, NCAR/TN-435-STR, 107, 1997.

20

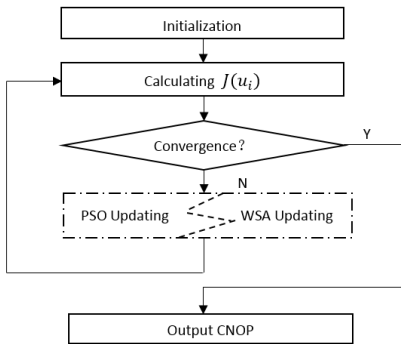


Figure 1: The framework of ACPW method.

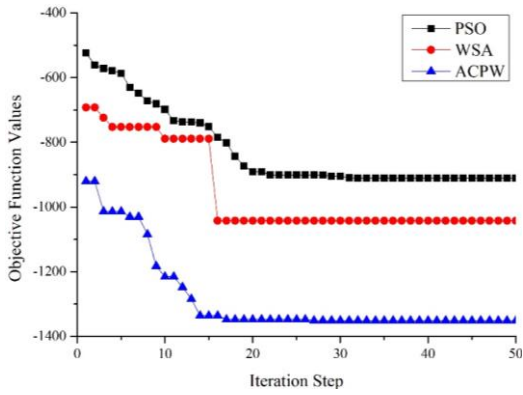
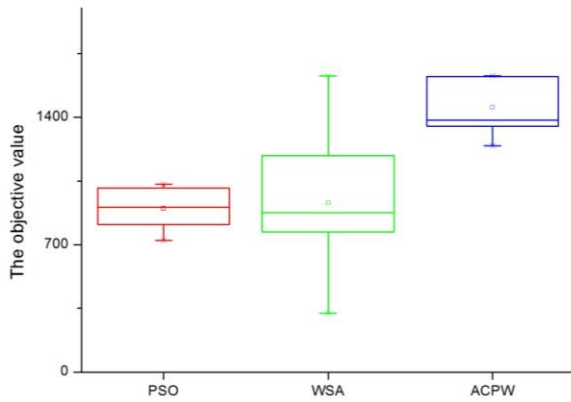


Figure 2: Convergence of the PSO, WSA and ACPW methods. PSO is denoted as the black line with squares, the WSA is shown as the red line with circles, and the ACPW algorithm is represented as the blue line with triangles.



5 Figure 3: The Box-plot of the PSO, WSA and ACPW methods for TC Fitow with the 60km at 60 km resolution. The red box denotes the PSO, the green box is for the WSA, and the blue box shows the results of the ACPW algorithm.

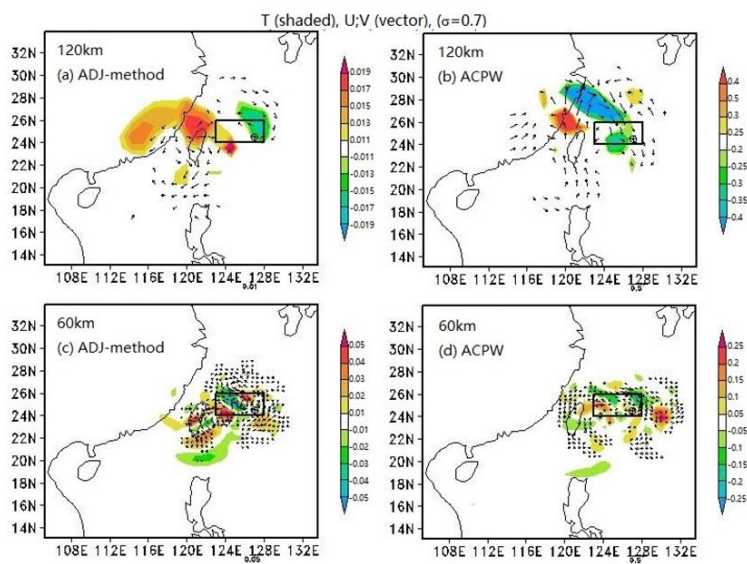


Figure 4: CNOP patterns at $\sigma=0.7$ for TC Fitow. The shaded parts represent the temperature (units: K), and the vectors describe the wind (units: m s⁻¹). The squares draw indicate the verification areas, and the initial cyclone positions are shown by \oplus . (a) and (b) denote the CNOP patterns with 120 km resolution for the ADJ-method and ACPW algorithm, respectively; (c) and (d) represent the CNOP patterns with 60 km resolution for the ADJ-method and ACPW algorithm, respectively.

带格式的: 英语(英国)

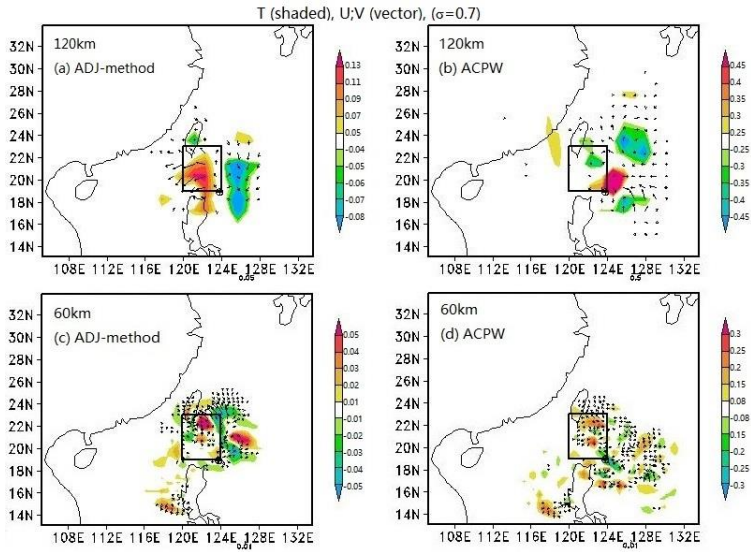


Figure 5: As in Fig. 3 except for tropical storm Matmo. The shaded parts represent the temperature (units: K) and the vectors describe the wind (units: m s⁻¹). The squares draw the verification areas and the initial cyclone positions are shown on ⊕. (a) and

(b) denote the CNOP patterns with

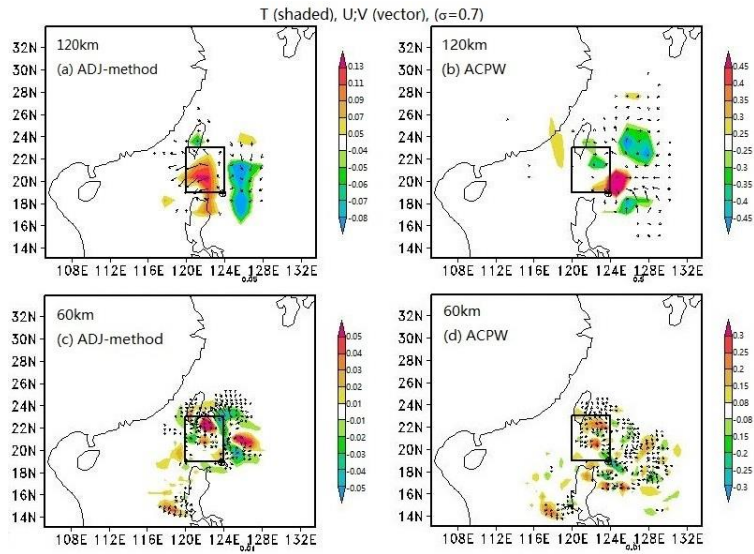


Figure 5: As in Fig. 3 except for tropical storm Matmo.

5 120 km resolution of ADJ-method and ACPW, respectively; (c) and (d) represent the CNOP patterns with 60 km resolution of ADJ-method and ACPW, respectively.

带格式的: 字体: 10 磅

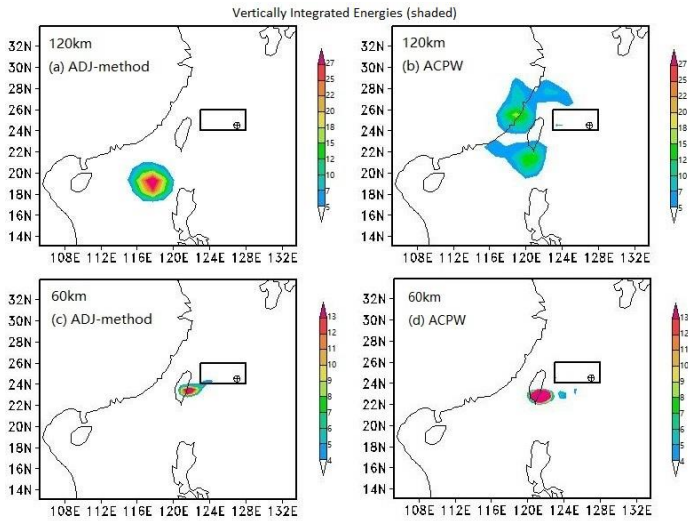


Figure 6: Same-as-As in Fig. 3, but except that the shaded parts represent the vertically integrated energies (units: $J\ kg^{-1}$).

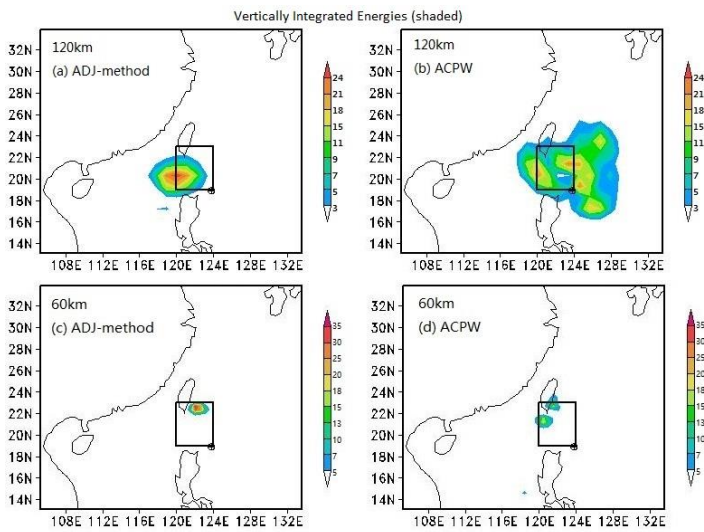


Figure 7: Same-as-As in Fig. 4, but except that the shaded parts represent the vertically integrated energies (units: $J\ kg^{-1}$).

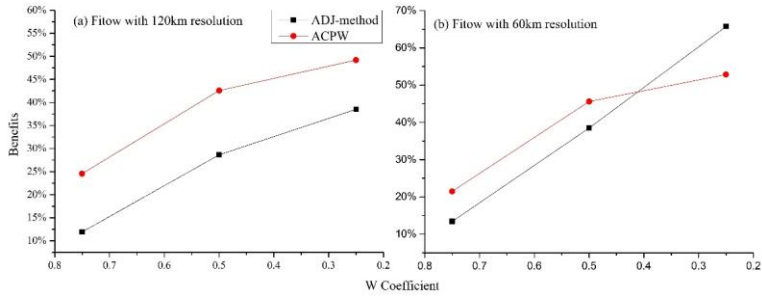


Figure 8: Benefits (percent, %) gained from reducing the CNOPs to $W \times$ CNOPs achieved by for the ADJ-method and ACPW in algorithm across the entire domain for TC Fitow (2013). The x-coordinate is the W coefficient values. And, and the y-coordinate denotes the benefits (percent, %) derived from the two methods. The ADJ-method is described presented as the black line with squares, and the ACPW result is the red line with circles.

5

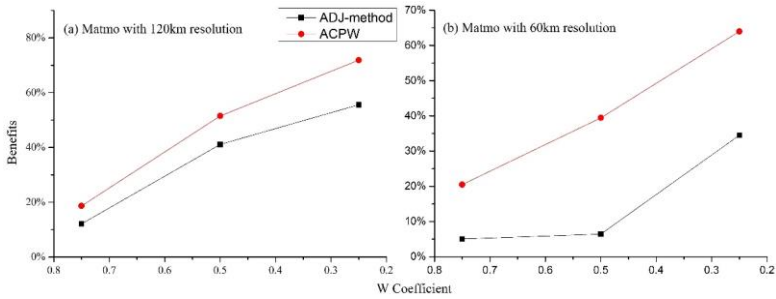


Figure 9: Benefits (percent, %) gained from by reducing the CNOPs to $W \times$ CNOPs identified by for the ADJ-method and ACPW in algorithm across the entire domain for TC Matmo (2014). The x-coordinate is the W coefficient values. And, and the y-coordinate denotes the benefits (percent, %) derived from the two methods. The ADJ-method is described presented as the black line with squares, and the ACPW result is the red line with circles.

10

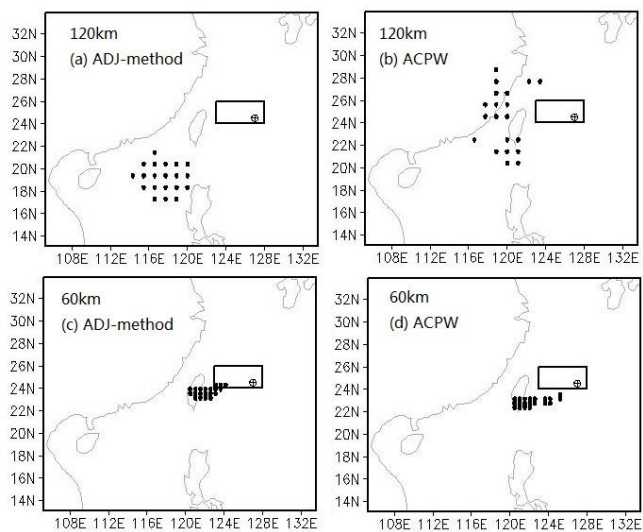


Figure 10: Sensitive regions identified by the CNOPs with 20 points for TC Fitw. The squares drawindicate the verification areas, and the initial cyclone positions are shown as \odot . (a) and (b) denote the CNOP patterns with 120 km resolution for the ADJ-method and ACPW algorithm, respectively; (c) and (d) represent the CNOP patterns with 60 km resolution for the ADJ-method and ACPW algorithm, respectively.

带格式的: 英语(英国)

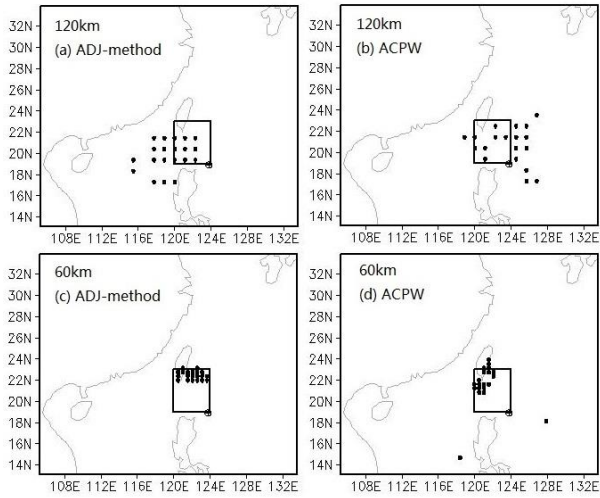


Figure 11: Sensitive regions identified by the CNOPs with 20 points for TC Matmo. The squares drawindicate the verification areas, and the initial cyclone positions are shown as \odot . (a) and (b) denote the CNOP patterns withat 120 km resolution efor the ADJ-method and ACPW algorithm, respectively; (c) and (d) represent the CNOP patterns withat 60 km resolution efor the ADJ-method and ACPW algorithm, respectively.

带格式的: 英语(英国)

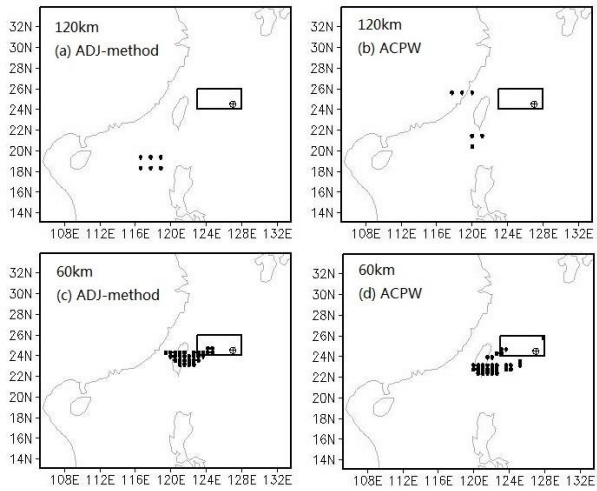
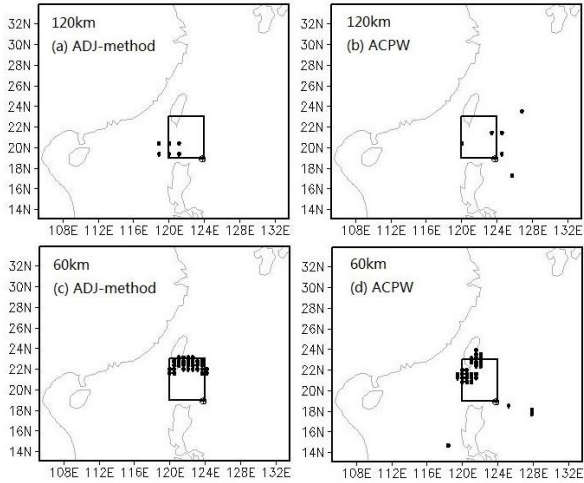


Figure 12: Sensitive regions identified by the CNOPs with 6 points **at** 120 km resolution and 30 points **at** 60 km resolution for TC Fitw. The squares **draw** indicate the verification areas, and the initial cyclone positions are shown **on** **the**. (a) and (b) denote the CNOP patterns **with** 120 km resolution **for** the ADJ-method and ACPW **algorithm**, respectively; (c) and (d) represent the CNOP patterns **with** 60 km resolution **for** the ADJ-method and ACPW **algorithm**, respectively.

带格式的: 英语(英国)



5

Figure 13: Sensitive regions identified by the CNOPs with 6 points **at** 120 km resolution and 30 points **at** 60 km resolution for TC Fitw. The squares **draw** indicate the verification areas, and the initial cyclone positions are shown **on** **the**. (a) and (b) denote the CNOP patterns **with** 120 km resolution **for** the ADJ-method and ACPW **algorithm**, respectively; (c) and (d) represent the CNOP patterns **with** 60 km resolution **for** the ADJ-method and ACPW **algorithm**, respectively.

带格式的: 英语(英国)

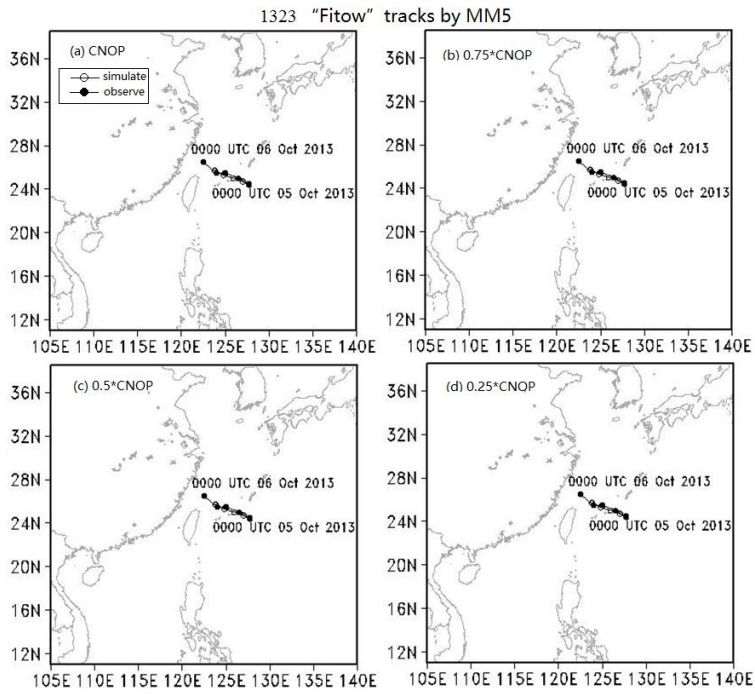


Figure 14: Simulated TC tracks offrom MM5 withby inserting CNOPthe CNOPs or $W \times \text{CNOP}$ into the initial state in the entire domain for TC Fitow. Solid circles represent the observed TC tracks offrom the CMA, and the hollow circles show the simulated TC tracks offrom the MM5 model. (a), (b), (c) and (d) denote the CNOP, $0.75 \times \text{CNOP}$, $0.5 \times \text{CNOP}$ and $0.25 \times \text{CNOP}$ results, respectively.

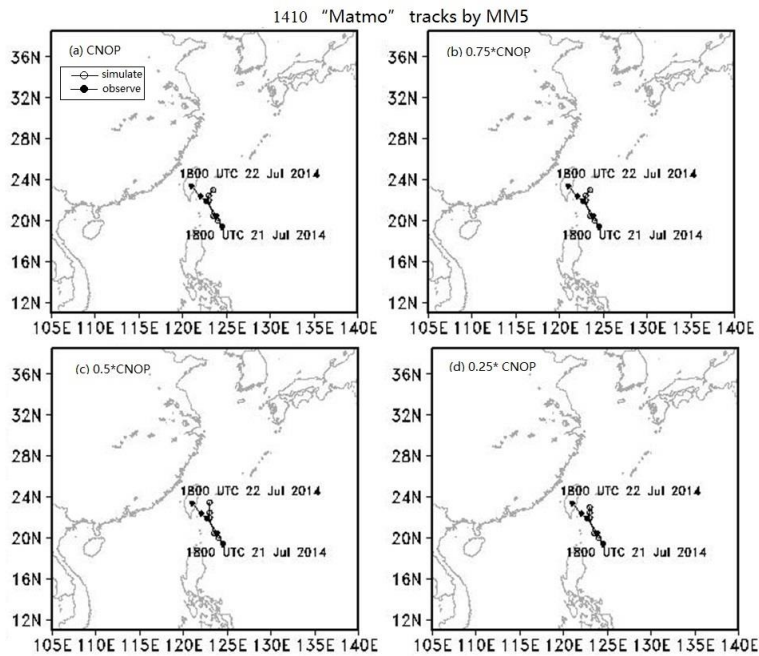


Figure 15: Simulated TC tracks offrom MMS withby inserting the CNOPs or $W \times \text{CNOP}$ into the initial state in the entire domain for TC Matmo. Solid circles represent observed TC tracks of CMA, and hollow circles show the simulated TC tracks of the MMS model. (a), (b), (c) and (d) denote CNOP, $0.75 \times \text{CNOP}$, $0.5 \times \text{CNOP}$ and $0.25 \times \text{CNOP}$, respectively.

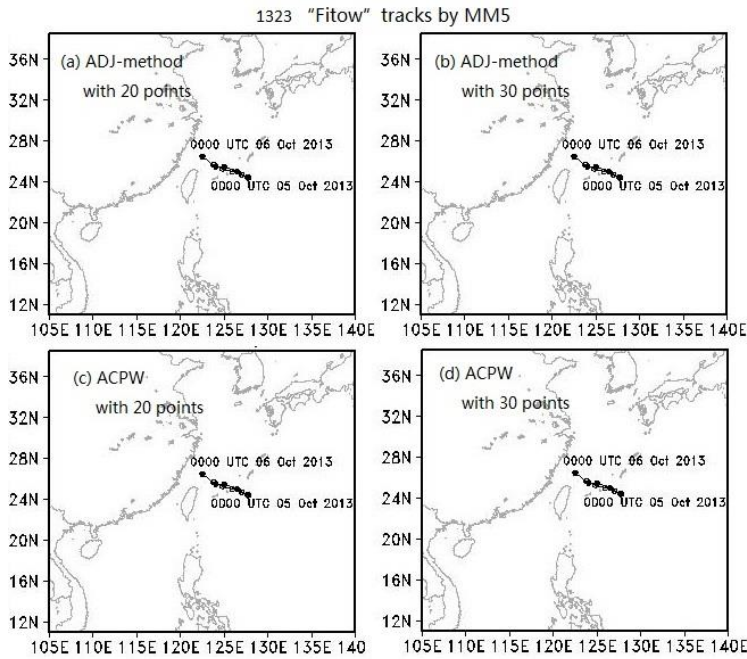


Figure 16: Simulated TC tracks from MMS withby inserting the amended CNOPs, which are reduced toby a factor of 0.5 time, in only in the sensitive regions, into the initial state for TC Fitow. Solid circles represent the observed TC tracks from the CMA, and the hollow circles show the simulated TC tracks from the MMS model. (a), (b), (c) and (d) denote the ADJ-method with 20 points, ADJ-method with 30 points, ACPW algorithm with 20 points and ACPW algorithm with 30 points, respectively.

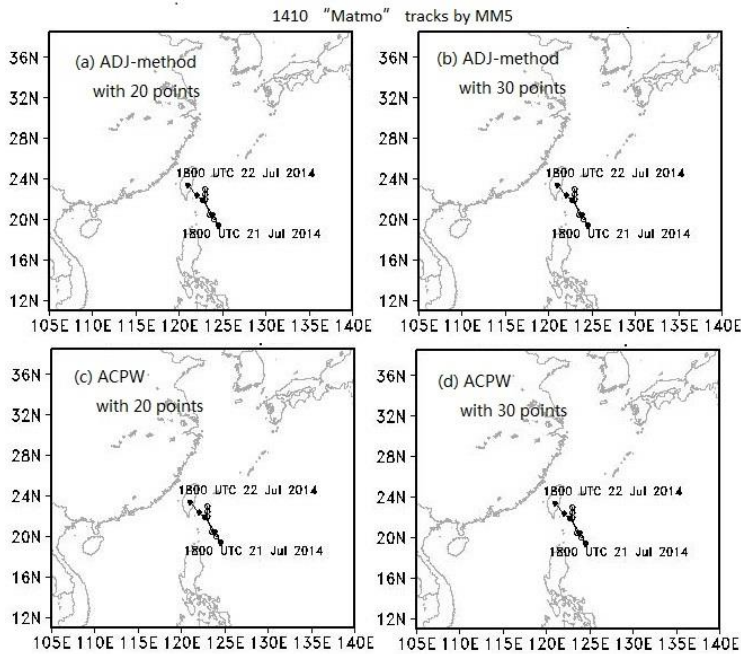


Figure 17: Simulated TC tracks ~~offrom~~ MM5 ~~withby~~ inserting ~~the~~ amended CNOPs, which are reduced ~~to~~ by a factor of 0.5 time, in only in the sensitive regions, into the initial state for TC Matmo. ~~Solid circles represent observed TC tracks of CMA, and hollow circles show the simulated TC tracks of the MM5-model.~~ (a), (b), (c) and (d) denote ADJ-method with 20 points, ADJ-method with 30 points, ACPW with 20 points and 30 points, respectively.

Table 1: ~~The parameters of ACPW.~~

Name	Meaning	Value
n	Number of principle components	50
N	Number of individuals	420 with 120kmat 120 km 200 with 60kmat 60 km
a	Adaptive coefficient	Initial: 0.5
ρ	Inertia coefficient	0.8
$c1$	Self-awareness to track the historically optimal position	2.05

带格式的: 英语(英国)

c_2	Social-awareness of the particle swarm to track the globally optimal position	2.05
γ	Restraint factor to control the speed	0.729
θ	Velocity of individual moving	0.5
r	Local optimizing radius	$8 \times \delta / \text{original dimensions}$
s	Step size of updating individual	0.6
p_a	Probability of individual escaping from current position	0.3
Total_Step	The number of iterations	50

Table 2: The meanings of all symbols.

Symbols	Values/ components	Meanings
δu_0	$u'_0, v'_0, T'_0, p'_{s0}$	Initial perturbation
u_{NT}	$u'_t, v'_t, T'_t, p'_{st}$	Nonlinear evolution of perturbed U_0 at time t
D	Values rely on cases	Verification area
σ	(0, 1]	Vertical coordinate
c_p	1005.7 J kg ⁻¹ K ⁻¹	Specific heat at constant pressure
R_a	287.04 J kg ⁻¹ K ⁻¹	Gas constant of dry air
T_r	270K	Constant parameter
p_r	1000hPa	Constant parameter

Table 3: The analysis results of the PSO, WSA and ACPW methods.

Algorithm	Max Value	Min Value	Mean Value	RMSE
PSO	1034.192573	724.086002	900.7488578	0.121400896
WSA	1628.841294	323.7493169	930.9103862	0.431193448
ACPW	2240.275956	1243.377921	1542.505251	0.216750584

Table 4: The similarities of CNOPs gained from ACPW and ADJ-method.

Table 4:

ACPW&/ADJ-method	120km	120 km	60km	60 km
------------------	-------	--------	------	-------

Fitow	-0.83	0.43
Matmo	0.42	0.37

Table 5: The ratios of energy for 24-h nonlinear evolutions with evolution by inserting the CNOPs-gained by from the ACPW algorithm and ADJ-method into the initial states.

ACPW/ADJ-method	120km120km	60km60 km
Fitow	94.1%	85.1%
Matmo	87.3%	70.2%

Table 6: Benefits (percent, %) gained from reducing the CNOPs to by a factor of 0.5 time in the sensitive regions identified by the ADJ-method and ACPW algorithm with 20 points.

Cases	Methods	60km60 km	120km120 km
Fitow	ADJ-method	3%	5.93%
	ACPW	-0.84%	8.05%
Matmo	ADJ-method	6.12%	20.90%
	ACPW	20.48%	16.26%

5 Table 7: Benefits (percent, %) gained from reducing the CNOPs to by a factor of 0.5 time in the sensitive regions identified by the ADJ-method and ACPW algorithm with 6 in 120km points at 120 km resolution and 30 points in 60km at 60 km resolution.

Cases	Methods	60km60 km (30 points)	120km120 km (6 points)
Fitow	ADJ-method	3.9	1.72%
	ACPW	4.23%	0.01%
Matmo	ADJ-method	1.21%	13.24%
	ACPW	9.75%	6.86%

Table 8: The time consumption of the ADJ-method and ACPW algorithm (unit: minutes).

Methods	60km60 km	120km120 km
ADJ-method (1) ¹	79.9	12.4
ADJ-method (4) ¹	321.1	49.7
ACPW	20.8	2.74

带格式的: 英语(英国)

带格式的: 英语(英国)

带格式的: 英语(英国)

带格式的: 英语(英国)

带格式的: 英语(英国)

带格式的: 字体: 10 磅

带格式的: 英语(英国)

带格式的: 英语(英国)